Bioorganic & Medicinal Chemistry 18 (2010) 6857–6864

Contents lists available at ScienceDirect

Bioorganic & Medicinal Chemistry

journal homepage: www.elsevier.com/locate/bmc

Structure–activity relationships of mononuclear metal–thiosemicarbazone complexes endowed with potent antiplasmodial and antiamoebic activities

Deepa Bahl [a], Fareeda Athar [b], Milena Botelho Pereira Soares [c,d], Matheus Santos de Sá [c], Diogo Rodrigo Magalhães Moreira [e], Rajendra Mohan Srivastava [e], Ana Cristina Lima Leite [f,*], Amir Azam [a,*]

[a] Department of Chemistry, Jamia Millia Islamia, Jamia Nagar, New Delhi 110025, India
[b] Centre for Interdisciplinary Research in Basic Sciences, Jamia Millia Islamia, New Delhi 110025, India
[c] Center of Research Gonçalo Moniz, Oswaldo Cruz Foundation, Rua Waldemar Falcão, 121, Candeal, Salvador 40296-710, BA, Brazil
[d] São Rafael Hospital, Av. São Rafael, 2152, São Marcos, Salvador 41253-190, BA, Brazil
[e] Department of Fundamental Chemistry, Centre for Natural Sciences (CCEN), Federal University of Pernambuco, 50740-540 Recife, PE, Brazil
[f] Department of Pharmaceutical Sciences, Centre for Health Sciences, Federal University of Pernambuco, 50740-520 Recife, PE, Brazil

ARTICLE INFO

Article history:
Received 10 July 2010
Accepted 16 July 2010
Available online 21 July 2010

Keywords:
Antiparasitic drugs
DNA
Entamoeba histolytica
Metal complexes
Plasmodium falciparum
Thiosemicarbazones

ABSTRACT

A useful concept for the rational design of antiparasitic drug candidates is the complexation of bioactive ligands with transition metals. In view of this, an investigation was conducted into a new set of metal complexes as potential antiplasmodium and antiamoebic agents, in order to examine the importance of metallic atoms, as well as the kind of sphere of co-ordination, in these biological properties. Four functionalized furyl-thiosemicarbazones (**NT1–4**) treated with divalent metals (Cu, Co, Pt, and Pd) to form the mononuclear metallic complexes of formula $[M(L)_2Cl_2]$ or $[M(L)Cl_2]$ were examined. The pharmacological characterization, including assays against *Plasmodium falciparum* and *Entamoeba histolytica*, cytotoxicity to mammalian cells, and interaction with pBR 322 plasmid DNA was performed. Structure–activity relationship data revealed that the metallic complexation plays an essential role in antiprotozoal activity, rather than the simple presence of the ligand or metal alone. Important steps towards identification of novel antiplasmodium (**NT1Cu**, IC_{50} of 4.6 μM) and antiamoebic (**NT2Pd**, IC_{50} of 0.6 μM) drug prototypes were achieved. Of particular relevance to this work, these prototypes were able to reduce the proliferation of these parasites at concentrations that are not cytotoxic to mammalian cells.

1. Introduction

According to the World Health Organization (WHO), there are 300–500 million clinical cases of malaria each year, resulting in an alarming rate of about 1.5–2.0 million deaths annually.[1] However, it is estimated that this death rate is likely to increase further because of the high level of drug resistance to most of the clinically used antimalarials.[2] Given the evidence of the global spread of drug resistance,[3] there is a need for the identification of new antiplasmodial drugs. After malaria, amebiasis (caused by *Entamoeba histolytica*) is the second leading cause of death from a protozoan parasite.[4] Metronidazole, the only WHO-recommended drug for treating amebiasis, is toxic and of questionable effectiveness in eliminating the parasite.[5] New safe and affordable amoebicidal drugs are therefore also urgently needed.

The elucidation of metabolic pathways of fundamental importance (e.g., fatty acid biosynthesis[6] and heme detoxification[7]) and of valid molecular targets, such as the falcipain-2,[8] CDK,[9] purine nucleoside phosphorylases,[10] and protein serine/threonine phosphatases[11] of *Plasmodium falciparum* have contributed to more rational design of drug candidates. In combination with this knowledge, the employment of modern concepts of medicinal chemistry, such as bioisosterism,[12] molecular hybridization,[13] bioinspired design in potent hit-compounds,[14] and the metallic complexation of plasmodicidal compounds[15] have accelerated the discovery of antiplasmodium drug candidates.

A significant number of transition metal-containing compounds have been either recently launched on the pharmaceutical market or entered into clinical trials, as exemplified by Ferrocifen, NAMI-A, Picoplatin, Ferroquine, and AMD3100.[16] In the specific case of antiplasmodium agents, in addition to Ferroquine that has recently entered in clinical trial, other metallic structures (complexes of co-ordination and organometallics) have shown promising in vitro and in vivo properties (Fig. 1).[17] It can thus be concluded that one successful drug development strategy is the complexation of transition metals with plasmodicidal agents, as it is possible to enhance the pharmacological and chemical properties (such as potency, selectivity, chemical stability, and lipophilicity) of the antiplasmodium agent employed.

* Corresponding authors. Tel.: +91 11 26981717x3250; fax: +91 11 26980229 (A.A.).
E-mail addresses: acllb2003@yahoo.com.br (A.C.L. Leite), amir_sumbul@yahoo.co.in (A. Azam).

0968-0896/$ - see front matter © 2010 Published by Elsevier Ltd.
doi:10.1016/j.bmc.2010.07.039

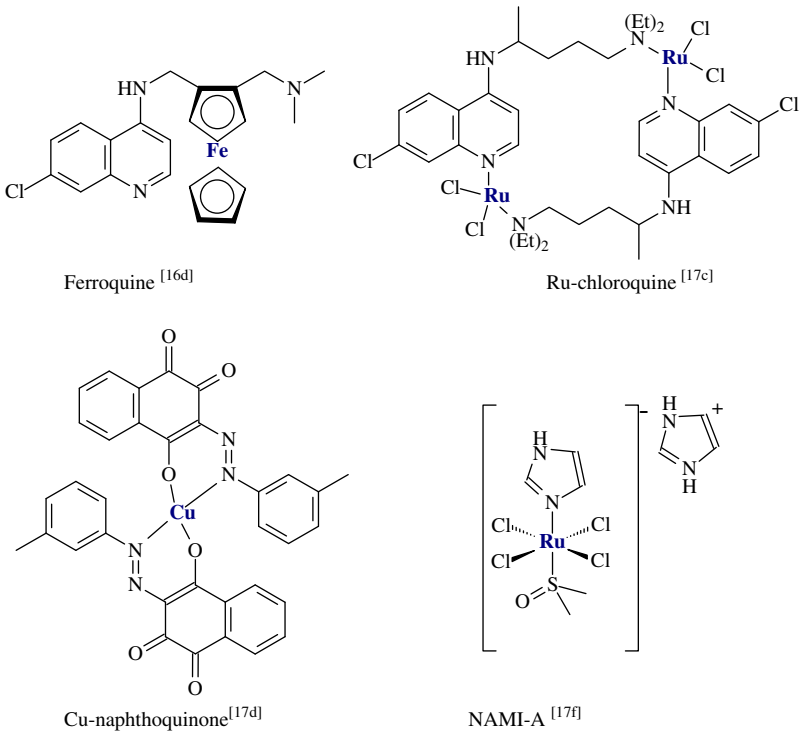

Figure 1. Examples of metallic compounds endowed with potent anti-*Plasmodium falciparum* activity.

Studies of thiosemicarbazone-based libraries have proved that they are useful ligands for the building of metal complexes with a wide variety of biological targets, including protozoan parasites.[8,18] Such ligands constitute an ideal source of bioactive ligands because they are endowed with the unique capacity of metallic co-ordination, semi-labile, chemically stables, and are synthetically treatable-features which make them suitable for performing structure–activity relationships (SAR) studies.[19] It is thus reasonable to believe that thiosemicarbazones are authentic privileged structures.[20]

According to this line of reasoning, metal–thiosemicarbazone complexes previously developed by us were found to improve anti-*E. histolytica* activity against the HK-9 and HM1:1MSS strains, when compared to the metal-free thiosemicarbazones.[21] On the one hand, we demonstrated that the cyclic bioisosters of thiosemicarbazones (thiocarboxamide-2-pyrazolines) are less effective against *E. histolytica* than thiosemicarbazones, suggesting that the replacement of a flexible backbone by a more rigid backbone results in a distinct interaction with the protozoan targets.[22] Moreover, insertion of bulk groups at the 4-position of thiosemicarbazones helps to improve the chemical stability of metal complexes and their lipophilicity, resulting in more potent antiamoebic complexes (Fig. 2).[23] Although there is a large number of thiosemicarbazones endowed with antiplasmodium activity,[24] investigations of the antiplasmodium activities for complexes of co-ordination containing thiosemicarbazones are scarce.[25]

In light of these findings, we decided to investigate the antiprotozoal properties of a new set of mononuclear metal–thiosemicarbazone complexes. In our design, the furfuryl ring was explored, in view of previous observation of its antiparasitic properties.[26] We have excluded attachment of the nitro group, as it is well-known that this induces toxicity, which is a drawback of the medicinal chemistry of antiparasitic drugs.[26c] Later, we selected platinum, palladium, cobalt, and copper, in search of complexes bearing one ($MLCl_2$) or two (ML_2Cl_2) ligands on each co-ordination sphere, thereby aiming to investigate how the ligand sphere contributes to antiprotozoal activity. Therefore, the main achievement of this study was to have gathered, for the first time, valuable SAR data on antiprotozoal metal–thiosemicarbazone complexes.

2. Results

2.1. Synthesis and general remarks of structural elucidation

The synthesis of ligands **NT1–4** was straightforward and proceeded moderate to good yields (41–90%). **NT1–4** were further used as chelating ligands to complex with $[Pd(DMSO)_2Cl_2]$, $[Pt(DMSO)_2Cl_2]$, $CoCl_2{\cdot}6H_2O$ or $CuCl_2{\cdot}2H_2O$ to generate the respective mononuclear metal–thiosemicarbazone complexes. Pt (**NT1Pt**, **NT2Pt**) and Pd (**NT1Pd**–**NT4Pd**) complexes were obtained as monomers by heating the ligand and appropriate metallic precursor under reflux, while the Co (**NT1Co**–**NT4Co**) and Cu

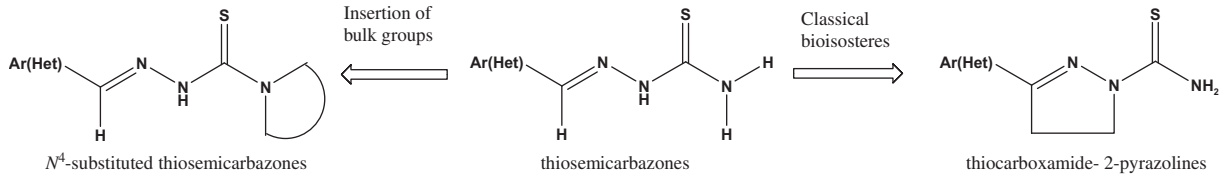

Figure 2. Our design concepts for thiosemicarbazones, their bioisosters classical (thiocarboxamide-2-pyrazolines) and their analogs containing bulk groups. Ar(Het) means either aromatic or heterocyclic rings.

(**NT1Cu**–**NT4Cu**) were obtained as bis-chelated complexes under similar conditions (Scheme 1). Elemental analysis data (C, H, N, and Cl) confirmed this metal–ligand ratio and accorded well with the calculated values.

The IR spectral signatures of **NT1–NT4** thiosemicarbazones show bands in the region at 1059–1109 cm^{-1} due to (νC=S), while no absorption appeared due to (νC–SH) in the region 2500–2600 cm^{-1}, suggesting that these **NT1–NT4** remain in its thione tautomeric form. For the metal complexes, although no shift was observed in the vibrations attributed to (νC–O–C) of furan ring, absorptions attributed to (νC=S) at 1059–1109 cm^{-1} were shifted to lower frequency (12–30 cm^{-1}) after the metallic complexation, indicating that thionic sulfur does participate in the sphere of co-ordination. More notably, strong bands at 1576–1603 cm^{-1} were observed in all the complexes, which can be attributed to chelation of (νC=N) with the metal.[19a,26b] By contrast, the (νCH=N) bands for the metal-free ligands are generally of higher frequency (1613–1615 cm^{-1}) and are of weaker intensity than those observed in the metal complexes. Bands observed in the region of 3100 cm^{-1} (νN–H) were also slightly shifted in the complexes, probably by any kind of adjustment of current around the thioamide group. Taking into account previous assignments for similar metal–thiosemicarbazone complexes, bands corresponding to metal-to-ligand stretching modes were tentatively assigned.[21] Thus, bands in the region of low wave-number (472–522 and 347–435 cm^{-1}) were assigned to νM–N and νM–S, respectively.

The ^{1}H NMR spectra of the ligands and their complexes were consistent with their corresponding protons both in terms of chemical shifts and the number of hydrogen atoms, in accordance with the proposed structure, allowing the assignment of each proton for the complexes. Regarding the ligands, it is worth reporting that even in DMSO-d_6 they were obtained in the thione form, which was confirmed by the absence of signal at ca. 4.0 ppm (–SH proton). Regarding the metallic complexes, the CH=N protons resonated at 6.6–7.3 ppm (singlet), owing to a deshielding effect observed for those protons that are in close proximity to the co-ordinating atoms (azomethine nitrogen), while, on free ligands, CH=N protons resonated at 7.8–8.0 ppm. On the basis of these comparisons, we suggest that an *N*,*S*-bidentate co-ordination is involved in these complexes, as proposed in Scheme 1.

Attempts to obtain single crystals of these metallic complexes suitable for X-ray diffraction were unsuccessful. To overcome this, additional analyzes were recorded and carefully studied. The mass spectra of the ligands and their metal complexes have showed the expected fragment ions, confirming the respective molecular weights. The overall splitting pathways of selected metal complexes are summarized in Supplementary data (Scheme S1). According to the electronic spectra, the **NT1–4** ligands exhibited three bands in the region at 220–207, 276–263, and 348–330 nm. The most probable assignments for these bands are the $n\rightarrow\pi^*$ (thiosemicarbazone), $\pi\rightarrow\pi^*$ (thiophene), and $\Phi\rightarrow\Phi^*$ (thiophene) transitions, respectively. A careful comparison of these bands with the electronic spectra of metallic complexes showed that there was an increase in intensity and a decrease in frequency due to the extended conjugation of ligands after the complexation. The observation of strong bands between 660 and 560 nm for the Pt (**NT1Pt**, **NT2Pt**) and Pd

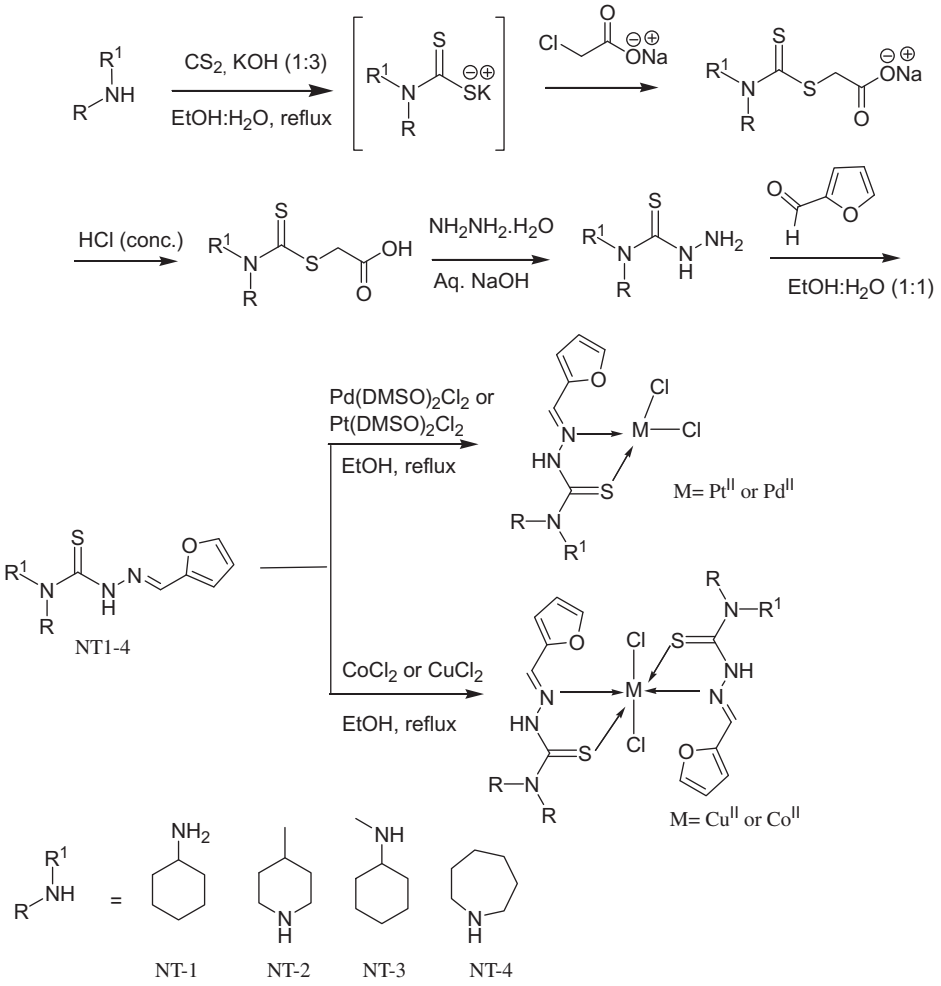

Scheme 1. Preparation of ligands (**NT1–4**) and their metal complexes.

(**NT1Pd–NT4Pd**) complexes were assigned to $^1A_1g \rightarrow 1A_{2g}$ that are typically of a square planar geometry. For these complexes, the ground state is ^1A_1g and the excited states are ^1A_2g, ^1B_1g, and ^1Eg in order of increasing energy. Intense bands were also observed at 433–470 nm and assignable to a combination of $S \rightarrow Pd^{II}$ and $^1A_{1g} \rightarrow {}^1B_{1g}$ transitions.[27] The Pt (**NT1Pt**, **NT2Pt**) and Pd (**NT1Pd–NT4Pd**) complexes were diamagnetic, as expected for a kind of complex that assumes the planar geometry.

For the Co (**NT1Co**–**NT4Co**) and Cu (**NT1Cu**–**NT4Cu**), two-spin was observed to allowed transitions at 575–550 nm and at 475–450 nm and attributed to $^4T_{1g}(F) \rightarrow {}^4T_{2g}(F)$ (ν_1) and $^4T_{1g}(F) \rightarrow 4T_{1g}(P)$ (ν_3). These transitions are suggestive of an octahedral geometry. Likewise, the ^2E_g and $^2T_{2g}$ microstates of the octahedral Cu^{II} ion (of configuration d^9) split under the influence of the tetragonal distortion and such distortion causes the transitions $^2B_{1g} \rightarrow {}^2B_{2g}$ and $^2B_{1g} \rightarrow {}^2A_{1g}$, although this remains unresolved in the electronic spectra.[28] These transitions lie within the single broad envelope centered on the range mentioned above. But these assignments accorded well with the general observation that transitions of the Cu^{II} d–d kind are often very similar in terms of energy.[29] The N–Cu^{II} and S–Cu^{II} ligand-to-metal charge transfer transitions were also observed at 460 nm (Table S1, supplementary data). The Cu and Co complexes exhibited room temperature magnetic moments (μ_{eff}) values in the range of 1.92–1.97 and 5.05–5.12 B.M., respectively (Table 1). These values are expected for magnetically diluted Cu^{II} and Co^{II} complexes having unpaired electrons in the d-orbital.[30]

The EPR spectra of the Cu^{II} and Co^{II} complexes were measured and the parameters are summed in Table 1. The general trend $g_{\|} > g_{\perp} > 2.0$ for the Cu complexes suggests that the unpaired electron is located on the $d(x^2 - y^2)$ ground state orbitals on the Cu^{II}[31] and can also be taken as evidence of an octahedral environment.[32] Likewise, the Co complexes exhibiting the g value between 2.05 and 2.08, which also suggests an octahedral environment around the metal.[33] To sum up, a square planar geometry is suggested for both the Pt^{II} (**NT1Pt**, **NT2Pt**) and Pd^{II} (**NT1Pd–NT4Pd**) complexes, while Cu^{II} complexes (**NT1Cu**–**NT4Cu**) and Co^{II} complexes (**NT1Co**–**NT4Co**) probably are of octahedral geometry.

These complexes are insoluble in water, sparingly soluble in methanol and ethanol, but soluble in DMF and DMSO, producing intense reddish, greenish or brownish solutions. The ^1H NMR spectra of metal complexes in DMSO-d_6 remained unchanged at room temperature for several days, showing no evidence of displacement of the thiosemicarbazones by the solvent. The solid-state geometry of dichloropalladium (**NT1Pd–NT4Pd**) and dichloroplatinum (**NT1Pt**, **NT2Pt**) complexes is not retained in DMSO solution, taking place an fast transformation of $[MLCl_2]$ to [ML(DMSO)Cl] complexes. All complexes were suspended in DMSO, thereby the biological activity reflects the presence of (DMSO)chlorometal complexes for the Pt and Pd ones.[34]

2.2. Pharmacological and physicochemical assays

All the ligands and complexes were tested against the erythrocytic stage (bloodstream form of clinical relevance) of *P. falciparum* (W2 clone, Chloroquine-resistant and Mefloquine-sensitive), HM-1:IMSS strain of *E. histolytica* trophozoites and also for cytotoxicity using BALB/c mouse splenocytes. The antiprotozoal properties were expressed in terms of the IC_{50} (μM) values, the cytotoxicity being expressed as the highest concentration tested that was non-cytotoxic for the splenocytes (Table 2). Mefloquine (**MQF**) and Metronidazole (**MNZ**) were used as reference drugs.

Recently, Sanchez-Delgado and co-workers have disclosed a number of correlations between physicochemical parameters and the antiplasmodium activity for a number of ruthenium–chloroquine complexes.[17c,35] From these studies, important insights into the antiplasmodium action mechanism were provided. Therefore, the saline/*n*-octanol partition coefficient (log *P*), studies with the pBR 322 plasmid DNA, and the inhibitory effects on the β-hematin formation for our most potent antiplasmodium metal–thiosemicarbazone complexes were also recorded (Table 3, Figs. 3 and 4).

2.3. Structure–activity relationships (SAR)

The first analysis of the pharmacological results showed that the **NT1–4** ligands were only weak *P. falciparum* inhibitors. Likewise, they were only modestly active against *E. histolytica*, the most potent being **NT2**, which is still four times less potent than **MNZ**. Although it was not possible to draw SAR data from these results, they displayed generally low cytotoxicity against mammalian cells, which suggests an attractive application for the building of metallic complexes.

As Cu complexes (**NT1Cu**–**NT4Cu**) are isoelectronic and isostructural with the Co complexes (**NT1Co**–**NT4Co**), while a square planar geometry is adopted by both Pt (**NT1Pt**, **NT2Pt**) and Pd (**NT1Pd–NT4Pd**) complexes, we concluded that the most appropriate discussion of the biological results is through the comparison between the similar metals, along the comparative analysis of the complex and the respective metal-free ligand.

Table 1
Analytical and physical data for the metal complexes

Compd	Color	Yield[a] (%)	Mp (°C)	(μ_{eff})[b]	EPR parameters[c]		
					$g_{\|}$	$g_{\perp}$	g
NT1Pt	Yellowish solid	34	260	0	—	—	—
NT2Pt	Pale yellow	43	200	0	—	—	—
NT1Pd	Pale orange	56	268	0	—	—	—
NT2Pd	Brick red	30	257	0	—	—	—
NT3Pd	Pale yellow	30	260	0	—	—	—
NT4Pd	Pale orange	55	220	0	—	—	—
NT1Co	Brownish solid	42	262	5.10	—	—	2.08
NT2Co	Wine red	35	165–170	5.05	—	—	2.05
NT3Co	Wine red	33	265	5.12	—	—	2.05
NT4Co	Chocolate brown	45	240	5.07	—	—	2.06
NT1Cu	Greenish solid	54	158	1.92	2.30	2.07	—
NT2Cu	Pale green	51	154	1.97	2.28	2.05	—
NT3Cu	Greenish solid	32	160	1.92	2.10	2.05	—
NT4Cu	Pale orange	40	164	1.95	2.20	2.06	—

[a] Isolated products.
[b] Effective magnetic moment expressed as Bohr Magneton (B.M.) and recorded at room temperature.
[c] From frozen solutions (77 K) in DMSO.

Table 2
Biological results of ligands and their metal complexes

Compd complexes	*P. falciparum* W2 strain IC_{50} (μM) after 24 h[a]	*E. histolytica* HM-1:IMSS strain IC_{50} (μM) after 72 h[a]	Cytotoxicity to mammalian cells (μg mL^{-1})[b]
NT1	20.3 ± 0.2	10.12 ± 00.5	33
NT2	36.2 ± 0.06	8.02 ± 00.1	100
NT3	21.8 ± 0.4	9.07 ± 00.4	>100
NT4	35.8 ± 0.9	12.08 ± 00.3	>100
NT1Pt	37.0 ± 0.1	3.47 ± 00.1	33
NT2Pt	42.3± 0.6	1.44 ± 00.3	>100
NT1Pd	10.0 ± 0.08	0.99 ± 00.3	3.3 (7.7)
NT2Pd	10.9 ± 0.1	0.6 ± 00.5	33
NT3Pd	18.3 ± 0.3	2.42 ± 00.5	33
NT4Pd	20.5 ± 0.01	1.66 ± 00.1	33
NT1Co	Nd	2.28 ± 00.1	33
NT2Co	41.0 ± 0.4	3.40 ± 00.2	33
NT3Co	21.4 ± 0.2	7.50 ± 00.5	33
NT4Co	58.7 ± 1.7	2.00 ± 00.3	100
NT1Cu	4.6 ± 0.1	1.11 ± 00.2	33
NT2Cu	5.2 ± 0.1	4.05 ± 00.1	11
NT3Cu	7.8 ± 2.0	1.80 ± 00.2	33
NT4Cu	4.6 ± 0.1	1.06 ± 00.4	3.3 (5.1)
MQN[c]	0.039 ± 0.01	–	N.d.
MNZ[c]	–	1.80 ± 00.3	N.d.

N.d., not determined at concentrations tested.
[a] Calculated from five concentrations using data obtained from at least three independent experiments. Values are mean ± standard deviation of three determinations.
[b] Expressed as the highest non-cytotoxic concentration for BALB/c mouse splenocytes. Values given in parentheses are expressed in μM.
[c] MQN is Mefloquine and MNZ is Metronidazole.

Table 3
Inhibitory effects on the β-hematin formation and partition coefficient (log *P*) for the copper complexes

Compd complexes	IC_{50} (μg mL^{-1})[a]	log *P*[b]
NT1Cu	>50	−1.73
NT2Cu	48	−1.54
NT3Cu	43	−1.49
NT4Cu	>50	−0.89
CP[c]	1.3	–

[a] Calculated from six concentrations using data obtained from two independent experiments. Values mean ±1.0.
[b] Performed as described in Section 4.
[c] CP is chloroquine diphosphate.

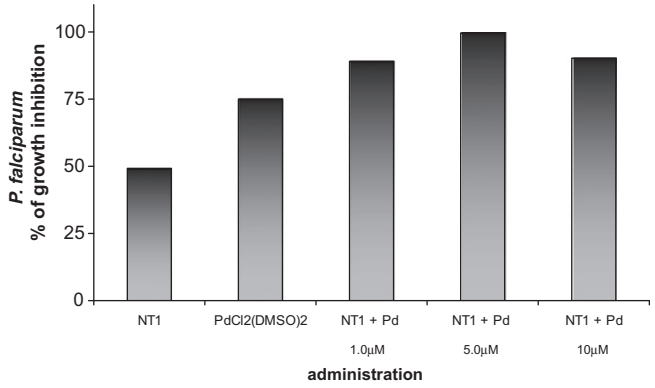

Figure 3. In vitro inhibition of *P. falciparum* growth at alone or concomitant addition of ligand (**NT1**) plus metal [$PdCl_2(DMSO)_2$, represented as Pd]. **NT1** was added at fix concentration of 20 μM, while Pd was used at 10 μM (alone) or at increasing concentrations (in concomitant with **NT1**). Data were measured in triplicate after 24 h of incubation, and the percentages of inhibitions were established in comparison to non-treated cells (control).

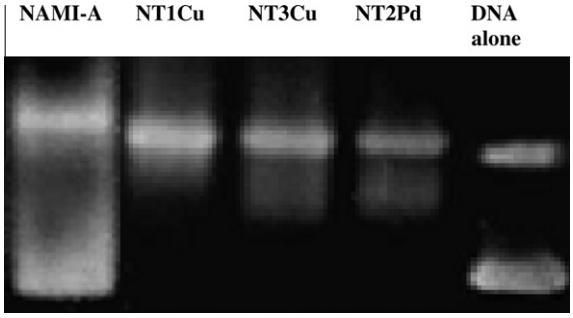

Figure 4. Effect of complexes **NAMI-A**, **NT1Cu**, **NT3Cu**, and **NT2Pd** (50 μM) on the mobility of pBR 322 plasmid DNA. DNA was incubated in 20 μM phosphate buffer (pH 7.5) to a final volume of 20 μL, and incubated in the absence or presence of tested complexes at 37 °C in the dark for 24 h.

We first analyzed the Pt and Pd series. Although the investigation of Pt complexes was limited by synthetic considerations and only two complexes (**NT1Pt** and **NT2Pt**) were prepared, these showed near IC_{50} values against *P. falciparum*. On the one hand, the Pt complexes showed improved potency against *P. falciparum* compared with than the metal-free ligands (**NT1** and **NT2**). On the other hand, the replacement of Pt by Pd led to only a slight increase in potency against *P. falciparum* (IC_{50} of 10.0–20.5 μM), far lower than the potency of **MQN**, which is active in nanomolar concentrations. Apart from **NT1Pd**, which was cytotoxic at low doses, the other Pt and Pd complexes retained their low cytotoxicity in mammalian cells. Noticeably, most of Pt and Pd complexes were highly potent in inhibiting the growth of *E. histolytica*, exhibiting the same range of potency as the reference drug, **MNZ**. A comparison of the inhibitory activity of ligand **NT2** and the **NT2Pd** complex, the latter proved to be 13 times more potent in inhibiting the proliferation of *E. histolytica*. By contrast, the replacement of ligand **NT2** by **NT3** resulted in the **NT3Pd** complex, which was only three times more potent than the free-ligand in inhibiting the growth of *E. histolytica*.

Regarding the antiplasmodial activity, the screening of Co and Cu complexes demonstrated more promising results than the Pt and Pd complexes. Analysis of these Co and Cu complexes bearing two molecules of ligands gave rise to interesting SAR observations. The complexation of **NT1–4** ligands with Co led a new set of

complexes that were (at least) one order of magnitude less active against *P. falciparum* (or in some cases virtually inactive, e.g., for **NT1Co** and **NT4Co**) when compared with the metal-free ligands. Conversely, the complexation with Co resulted in antiamoebic complexes more potent than the corresponding metal-free ligands.

Regarding the metal-free thiosemicarbazones (IC_{50} of 20.3–36.2 μM), their Cu complexes were proven to be good antiplasmodial agents (IC_{50} of 4.6–7.8 μM), exhibiting the following order of potency: **NT1Cu** = **NT4Cu** > **NT2Cu** > **NT3Cu**. Altering the structure of the cyclohexyl ring on the ligands of *C*-methyl (**NT2Cu**) to *N*-methyl (**NT3Cu**) led to a slight reduction in potency (IC_{50} = 5.2 vs 7.8 μM). Moreover, it was observed that, although the ring expansion of cyclohexyl (**NT1Cu**) by cycloheptane (**NT4Cu**) retains the antiplasmodial activity, **NT4Cu** was cytotoxic against mammalian cells.

2.4. Advanced biological experiments

On the basis of the SAR data presented in Table 2, it seems that the antiplasmodial activity of these complexes is dependent on the substituents (R) on the structures of thiosemicarbazones (**NT1–4**). In general, the lipophilicity of metallic structures is a relevant descriptor for explaining the cell uptake, and for explaining the difference in potency between the metal complex and its metal-free ligand. In the case of anti-malarial complexes, such as Ferroquine[16d] and ruthenium–chloroquine,[17c,35] the antiplasmodium activity is governed by the influence of lipophilicity. The lipophilicity (log *P*) of our most potent antiplasmodium complexes (**NT1Cu**–**NT4Cu**) was thus measured, in order to check any kind of correlation with the biological activity. Comparing the experimental values of log *P* (Table 3) with the IC_{50} values against the W2 strain *P. falciparum*, a correlation between the potency and lipophilicity is not observed. However, comparing the lipophilicity of **NT1** (log *P* = 2.16) ligand and its copper complex (**NT1Cu**), it is possible to conclude that the copper complexes are in fact more hydrophilic than the free thiosemicarbazones.

To ascertain whether complexation with a ligand is an essential factor for antiprotozoal activity, the same culture of W2 strain *P. falciparum* was simultaneously treated with stoichiometric quantities (20 μM) of metal-free ligand **NT1** and its metallic precursor $[PdCl_2(DMSO)_2]$, with the percentage of cell growth inhibition being measured after 24 h of treatment. In this condition, only 56% of the *P. falciparum* proliferation was inhibited, approximately twice lower than that of the corresponding **PdNT1** complex (98% of inhibition at 20 μM). Since the bioactivity of simultaneously treatment (ligand plus metallic precursor) and its corresponding metallic complex are distinct, the antiplasmodium activity of these complexes is not governed by synergistic effects alone. Cumulatively, it is supposed that the formation of a metal complex, rather than the simple presence of the ligand or transition metal alone, plays a crucial role in determining its antiprotozoal properties.

Regarding the lability of thiosemicarbazones, Bernhardt and coworkers have proposed that thiosemicarbazones from metallic complexes are displaced (dissociated) under physiological conditions or, in other words, the metals act as lipophilic vehicles, facilitating the intracellular delivery of the metal-free thiosemicarbazones into cellular compartments.[19b,c] In light of these findings, it is supposed that the processes of precomplexation and dissociation play a pivotal role in determining the pharmacological potency for the metallic complexes described here. To gather additional evidences, additional biological assays were performed with palladium, which is kinetically more labile than Cu, Co, or Pt.

The same culture of W2 strain *P. falciparum* was simultaneously treated with metal-free ligand **NT1** (20 μM) and its metallic precursor $[PdCl_2(DMSO)_2]$ at increasing concentrations (1.0, 5.0, and 10 μM), with the percentage of cell growth inhibition being measured after 24 h of treatment. From the data on Figure 3, it is possible to suggest that the increasing addition of Pd enhances the antiplasmodium activity of **NT1** ligand at certain point. However, at high concentrations of Pd (more than 10 μM), no differences of inhibitions are observed, may because of metal toxicity (data not shown). Although preliminary, the role of metal facilitating the intracellular delivery of thiosemicarbazones into cellular compartments may occur in the complexes described here, providing a means for drug activation or formation of reactive species that could eventually interact with the protozoan targets.

As previously cited, there are various examples of drug targets of *P. falciparum*. Following the findings provided by Sanchez-Delgado and co-workers, the DNA and hematin were considered as potential drug targets.[35] Therefore, studies of DNA interaction in cell-free media was conducted, employing pBR 322 plasmid DNA (composed of the supercoiled form of higher mobility and an open circular relaxed form) and CT-DNA (denatured form). We chose three of the most potent and non-cytotoxic complexes to be tested, **NT1Cu**, **NT3Cu**, and **NT2Pd**. These complexes are insoluble in pure water, and DMSO was thus used as a co-solvent in concentrations that do not affect the CT-DNA. The addition of the metal complexes to the CT-DNA solution resulted in small changes in the UV–vis absorption spectra. The observed changes were almost identical in the presence of each of these three complexes, suggesting that the complexes interact with CT-DNA in the same way (data not shown).

More valuable informations were gathered by way of agarose gel electrophoresis assays using pBR 322 plasmid DNA. In this assay, the NAMI-A (an imidazole–ruthenium^{II} complex, Fig. 1) of recognized in vitro antiplasmodium property[17e] was used, so as to establish a point of reference for the metal entity. At concentrations below 50 μM, the complexes (**NT1Cu**, **NT3Cu**, and **NT2Pd)** did not alter either the migration of plasmid DNA bands or other interaction processes (cleavage, for instance) to a significant degree, while the NAMI-A showed interactions as soon as a concentration of 10 μM was reached. However, at 50 μM, a new pattern was observed after the incubation of these complexes with plasmid DNA. Figure 4 suggests that the DNA interaction of these complexes occurs through the conversion of the supercoiled form, probably to the relaxed form, while the NAMI-A-treated DNA behaved quite differently, exploiting the cleavage process.

Inhibition of β-hematin formation was also measured for our more potent copper complexes (Table 3). All the tested complexes did not inhibit the β-hematin formation to a significant extent, while chloroquine did. This suggests these complexes use a different action mechanism than quinoline-based antimalarial drugs. In view of the current problem of resistance to anti-malarial drugs,[3] it is especially important to identify novel anti-malarial drug candidates not based on quinolines.

As a result of these assays, the plasmodicidal action mechanism must, in part, be related to action on the DNA structure. As for the antiamoebic properties of these metal complexes, it is not clear whether the antiamoebic action mechanism involves their interaction with DNA. Although additional experimental data is not available at present, a very recent survey of the literature indicates that the sequestration of Fe via either chelator compounds or exchange of endogenous Fe by exogenous metal (transmetalation) affects *E. histolytica* viability.[36] In light of these studies, it is reasonable to propose that, given the recognized ability of thiosemicarbazones to act as Fe chelators, as well as the feasibility of the complexes described here to participate in the processes of dissociation, they may use this action mechanism to inhibit the growth of *E. histolytica*.

3. Conclusions

We were able to identify **NT2Pd** as the most potent antiamoebic agent tested in this study, being twice as effective as **MNZ**. **NT2Pd**

did not show cytotoxicity against splenocytes at a concentration 10 times higher than that capable of inhibiting *E. histolytica* growth. In other words, it was effective at concentrations that do not overtly affect mammalian cells. This represents the kind of profile, that is, generally required for antiparasitic agents, with selective toxicity against parasites, although future investigations in animal models are necessary.

Our most potent antiplasmodial complex, **NT1Cu**, is far less potent than **MNQ**. However, the copper complexes, particularly **NT1Cu** and **NT2Cu**, represent good starting points for further medicinal chemistry programs aiming to discover antimalarial drug candidates based on metallic structures. Our future goals are to study Pd and Cu complexes bearing mixed-ligands to further validate the hypothesis that the process of dissociation may occur and could be exploited to produce complexes more active complexes against the aforementioned parasites.

4. Experimental section

4.1. Chemistry

General remarks: reactions were monitored by TLC analysis using Merck pre-coated aluminum plate silica gel $60F_{254}$ thin layer plates. All the chemicals were purchased from Aldrich Chemical Company (USA). Elemental analysis (C, H, N) was carried out by Central Drug Research Institute, Lucknow (India). Chlorine was estimated by decomposing the complexes with Na_2O_2/NaOH and precipitating as AgCl with $AgNO_3$ after dissolving in diluted HNO_3. Melting points were recorded on KSW melting point apparatus and are uncorrected. Electronic spectra were recorded in methanol on a Shimadzu UV-1601 PC UV-visible spectrophotometer. IR spectra on KBr disks were recorded on a Perkin Elmer model 1620 FT-IR spectrophotometer. ^{1}H NMR spectra were obtained at ambient temperature using a Brucker spectroscopin DPX-300 MHz spectrophotometer in DMSO-d_6 using TMS as an internal standard. Splitting patterns are designated as follows: s, singlet, d, doublet, m, multiplet. The FAB mass spectra of all the complexes were recorded on a JEOL SX 102/DA-6000 Mass Spectroscopy/Data System, using argon/xenon (6 kV, 10 mA) as the FAB gas and *m*-nitrobenzyl alcohol (NBA) as the matrix. Room temperature magnetic susceptibility was measured at 298 K by a Vibrating sample Magnetometer 155, E-112 ESR Spectrometer, Varian, USA using nickel as standard and such values were expressed as effective magnetic moment (μ_{eff}) in Bohr Magneton (B.M.). The electron paramagnetic resonance (EPR) spectra were recorded with a Bruker ESP 300E X-band spectrometer.

4.1.1. Synthesis of ligands

The thioglycolic acids were prepared as outlined in reference.[37] The thiosemicarbazones were synthesized by heating at reflux an aqueous solution of respective aminothiocarbonylhydrazines (0.003 mol in 10 mL) with ethanolic solution of furan-2-carboxaldehyde (0.228 g, 0.003 mol in 10 mL) for 3 h with continuous stirring. After cooling, the precipitated compound was filtered and recrystallized from appropriate solvent.

4.1.2. Synthesis of Pd^{II} and Pt^{II} complexes of thiosemicarbazones

The synthesis of Pd^{II} and Pt^{II} complexes [$M(DMSO)_2Cl_2$, where M is Pd or Pt] were prepared in accordance the procedure outlined in the literature.[38] A solution of [$Pd(DMSO)_2Cl_2$]/[$Pt(DMSO)_2Cl_2$] (2 mmol) dissolved in methanol (5 mL) was added to a solution of respective ligand (2 mmol) previously dissolved in a minimum quantity of methanol and the reaction mixture was heated under reflux for 1–3 h. After keeping the solution at 0 °C overnight, the colored solid was filtered out. This was washed with hot water followed by a small quantity of methanol and dried in a vacuum desiccator over anhydrous silica gel to give amorphous solids.

4.1.3. Synthesis of Cu^{II} and Co^{II} complexes of thiosemicarbazones

A stirred solution of hydrated metal chloride (2 mmol) dissolved in minimal quantity of methanol was added to a stirring hot solution of ligand (4 mmol) in methanol (20 mL) and the reaction mixture was heated under reflux for 1–3 h. This solution was kept to room temperature overnight, when the precipitate was filtered out, washed with hot water followed by small quantity of methanol, and dried. Recrystallization was carried out from methanol.

4.2. Pharmacological procedures

4.2.1. Cytotoxicity to mammalian cells

The cytotoxicity of the compounds and metal complexes was determined using BALB/c mouse splenocytes (5×10^6 cells well^{-1}) cultured in 96-well plates in Dulbecco's Modified Eagle's Medium (DMEM, Sigma Chemical Co., St. Louis, MO) supplemented with 10% of fetal calf serum (FCS; Cultilab, Campinas, SP, Brazil) and 50 μg mL^{-1} of gentamycin (Novafarma, Anápolis, GO, Brazil). Each compound was evaluated in five concentrations (1.1, 3.3, 11, 33, and 100 μg mL^{-1}), in triplicate. Cultures were incubated in the presence of ^{3}H-thymidine (1 μCi well^{-1}) for 24 h at 37 °C and 5% CO_2. After this period, the content of the plate was harvested to determine the ^{3}H-thymidine incorporation using a β-radiation counter (Multilabel Reader, Hidex, Turku, Finland). The cytotoxicity of the compounds was determined comparing the percentage of ^{3}H-thymidine incorporation (as indicator of viability cell) of drug-treated wells in relation to untreated wells. Non-cytotoxic concentrations were defined as those causing a reduction of ^{3}H-thymidine incorporation below 10% in relation to untreated controls. *Note*: BALB/c mice were handled according to the NIH guidelines for animal experimentation. All procedures described here had prior approval from the animal ethics committee of FIOCRUZ (Brazil).

4.2.2. Antimalarial activity

It was performed using the [^{3}H]-hypoxanthine incorporation assay, as previously described.[39] Briefly, parasites were maintained in continuous culture of human erythrocytes (blood group O^+) using RPMI 1640 medium supplemented with 10% human plasma. Parasites grown at 1–2% parasitemia and 2.5% hematocrit were incubated with the pure substances tested at five different concentrations, diluted with 4% DMSO in culture medium (RPMI 1640) without hypoxanthine. Cultures containing parasites were harvested using a cell harvester to evaluate the [^{3}H]-hypoxanthine incorporation in a β-radiation counter. Inhibition of parasite growth was evaluated by comparison with [^{3}H]-hypoxanthine uptake in drug treated versus untreated wells after 24 h of incubation with the tested compounds. IC_{50} values were calculated triplicates, comparing with the Mefloquine (**MQN**) as standard drug.

4.2.3. Antiamoebic activity

Thiosemicarbazones and their metal complexes were screened against the HM-1:IMSS strain of *E. histolytica* by using the microplate method.[40] All the experiments were carried out in triplicates at each concentration level and repeated thrice. *E. histolytica* trophozoites were cultured in TYI-S-33 growth medium in wells of 96 well microtiter plates.[41] DMSO (40 μL) was added to all the samples (1 mg) followed by enough culture medium to obtain concentration of 1 mg/mL. The maximum concentration of DMSO in the test did not exceeded 0.1%, and at this level no inhibition of amoebal growth has occurred. Compounds were further diluted with medium to a concentration of 0.1 mg mL^{-1}. Twofold serial

dilutions were made in the wells of 96-well microtiter plate. Each test included Metronidazole (MNZ) as the standard amoebicidal drug, control (culture medium plus parasite) and a blank (culture medium only). The cell suspension was then diluted to 10^5 organism/mL by adding fresh medium and 170 μL of this suspension was added to the test and control well in the plate. Plate was sealed and gassed for 10 min with nitrogen before incubation at 37 °C for 72 h. After incubation, the growth of amoebae in the plate was checked with a low power microscope and the optical density of the solution in each well was determined at 490 nm with a microplate reader. The% inhibition of amoebal growth was calculated from the optical densities of the control and test wells and plotted against the logarithm of the dose of the drug tested. Linear regression analysis was used to determine the best-fitted straight line from which the IC_{50} value was found.

Acknowledgements

This study received support from Council of Scientific and Industrial Research (grant #01(2278)/08/EMR-II New Delhi, India), Pernambuco State Foundation of Science (FACEPE, grant #APQ-0123-4.03/08, Brazil), and Bahia State Foundation of Science (FAPESB, PRONEX project, Brazil). Diogo Moreira holds a CNPq scholarship. The authors acknowledge the technical assistance of José Fernando Costa (FIOCRUZ, Brazil) in the cytotoxicity assays.

Supplementary data

Supplementary data (compound characterization of the compounds outlined in Scheme 1. Pharmacological protocols conducted can also be found in the Supporting Information) associated with this article can be found, in the online version, at doi:10.1016/j.bmc.2010.07.039.

References and notes

1. World Health Organization Reports, last access in April 2010, at http://www.who.int/malaria/en/.
2. Mahomva, A. I.; Peterson, D. E.; Rakata, L. *Cent. Afr. J. Med.* **1996**, *42*, 345.
3. Bustamante, C.; Batista, C. N.; Zalis, M. *Curr. Drug Targets* **2009**, *10*, 279.
4. Stanley, S. L., Jr. *Lancet* **2003**, *361*, 1025.
5. (a) Adagu, I. S.; Nolder, D.; Warhurst, D. C.; Rossignol, J. F. *J. Antimicrob. Chemother.* **2002**, *49*, 103; (b) Singh, S.; Bharti, N.; Mohapatra, P. P. *Chem. Rev.* **2009**, *109*, 1900.
6. Lu, J. Z.; Lee, P. J.; Waters, N. C.; Prigge, S. T. *Comb. Chem. High Throughput Screen.* **2005**, *8*, 15.
7. Tekwani, B. L.; Walker, L. A. *Comb. Chem. High Throughput Screen.* **2005**, *8*, 63.
8. Kerr, I. D.; Lee, J. H.; Farady, C. J.; Marion, R.; Rickert, M.; Sajid, M.; Pandey, K. C.; Caffrey, C. R.; Legac, J.; Hansell, E.; McKerrow, J. H.; Craik, C. S.; Rosenthal, P. J.; Brinen, L. S. *J. Biol. Chem.* **2009**, *284*, 25697.
9. Canduri, F.; Perez, P. C.; Caceres, R. A.; Azevedo, W. F., Jr. *Curr. Drug Targets* **2007**, *8*, 389.
10. Silva, R. G.; Nunes, J. E.; Canduri, F.; Borges, J. C.; Gava, L. M.; Moreno, F. B.; Basso, L. A.; Santos, D. S. *Curr. Drug Targets* **2007**, *8*, 413.
11. Bajsa, J.; Duke, S. O.; Tekwani, B. L. *Curr. Drug Targets* **2008**, *9*, 997.
12. Lima, L. M.; Barreiro, E. J. *Curr. Med. Chem.* **2005**, *12*, 23.
13. Viegas-Junior, C.; Danuello, A.; Bolzani, V. S.; Barreiro, E. J.; Fraga, C. A. M. *Curr. Med. Chem.* **2007**, *14*, 103.
14. Gelb, M. H.; Van Voorhis, W. C.; Buckner, F. S.; Yokoyama, K.; Eastman, R.; Carpenter, E. P.; Panethymitaki, C.; Brown, K. A.; Smith, D. F. *Mol. Biochem. Parasitol.* **2005**, *126*, 155.
15. Sanchez-Delgado, R. A.; Anzellotti, A. *Mini. Rev. Med. Chem.* **2004**, *4*, 23.
16. For excellent reviews of bioactive metallic structures, see: (a) Beraldo, H.; Gambino, D. *Mini. Rev. Med. Chem.* **2004**, *4*, 31; (b) Storr, T.; Thompson, K. H.; Orvig, C. *Chem. Soc. Rev.* **2006**, *35*, 534; (c) Fricker, S. P. *Dalton Trans.* **2007**, 4903; (d) Dive, D.; Biot, C. *ChemMedChem* **2008**, *3*, 383.
17. A survey of metallic structures endowed with antiplasmodium properties: (a) Sanchez-Delgado, R. A.; Navarro, M.; Perez, H.; Urbina, J. A. *J. Med. Chem.* **1996**, *39*, 1095; (b) Harpstrite, S. E.; Beatty, A. A.; Collins, S. D.; Oksman, A.; Goldberg, D. E.; Sharma, V. *Inorg. Chem.* **2003**, *42*, 2294; (c) Navarro, M.; Vasquez, F.; Sanchez-Delgado, R. A.; Perez, H.; Sinou, V.; Schrevel, J. *J. Med. Chem.* **2004**, *47*, 5204; (d) Gokhale, N. H.; Shirisha, K.; Padhye, S. B.; Croft, S. L.; Kendrick, H. D.; Mckee, V. *Bioorg. Med. Chem.* **2006**, *16*, 430; (e) Martínez, A.; Rajapakse, C. S. K.; Naoulou, B.; Kopkalli, Y.; Davenport, L.; Sanchez-Delgado, R. A. *J. Biol. Inorg. Chem.* **2008**, *13*, 703; (f) Gabbiani, C.; Messori, L.; Cinellu, M. A.; Casini, A.; Mura, P.; Sannella, A. R.; Severini, C.; Majori, G.; Bilia, A. R.; Vincieri, F. F. *J. Inorg. Biochem.* **2009**, *103*, 310; (g) Schuh, E.; Valiahdi, S. M.; Jakupec, M. A.; Keppler, B. K.; Chiba, P.; Mohr, F. *Dalton Trans.* **2009**, 10841; (h) Rajapakse, C. S. K.; Martinez, A.; Naoulou, B.; Jarzecki, A. A.; Suarez, L.; Deregnaucourt, C.; Sinou, V.; Schrevel, J.; Musi, E.; Ambrosini, G.; Schwartz, G. K.; Sanchez-Delgado, R. A. *Inorg. Chem.* **2009**, *48*, 1122; (i) Adediji, J. F.; Olayinka, E. T.; Adebayo, M. A.; Babatunde, O. *Int. J. Phys. Sci.* **2009**, *4*, 529; (j) Soares, M. B. P.; Costa, J. F. O.; de Sá, M. S.; Ribeiro-dos-Santos, R.; Jaouen, G.; Santana, A. E. G.; Goulart, M. O. F.; Hillard, E. *Drug Dev. Res.* **2010**, *71*, 69.
18. (a) Cerecetto, H.; Gonzalez, M. *Mini Rev. Med. Chem.* **2008**, *8*, 1355; (b) Donnici, C. L.; Araújo, M. H.; Oliveira, H. S.; Moreira, D. R. M.; Pereira, V. R. A.; Souza, M. de A.; De Castro, M. C. A. B.; Leite, A. C. L. *Bioorg. Med. Chem.* **2009**, *17*, 5038.
19. (a) Rebolledo, A. P.; Vieites, M.; Gambino, D.; Piro, O. E.; Castellano, E. E.; Zani, C. L.; Souza-Fagundes, E. M.; Teixeira, L. R.; Batista, A. A.; Beraldo, H. *J. Inorg. Biochem.* **2005**, *99*, 698; (b) Yu, Y.; Kalinowski, D. S.; Kovacevic, K.; Siafakas, A. R.; Jansson, P. J.; Stefani, C.; Lovejoy, D. B.; Bernhardt, P. V.; Richardson, D. R. *J. Med. Chem.* **2009**, *52*, 5271; (c) Bernhardt, P. V.; Sharpe, P. C.; Islam, M.; Lovejoy, D. B.; Kalinowski, D. S.; Richardson, D. R. *J. Med. Chem.* **2009**, *52*, 407.
20. Duarte, C. D.; Barreiro, E. J.; Fraga, C. A. M. *Mini Rev. Med. Chem.* **2007**, *7*, 1108.
21. (a) Shailendra, N.; Bharti, N.; Naqvi, F.; Azam, A. *Bioorg. Med. Chem. Lett.* **2003**, *13*, 689; (b) Singh, S.; Athar, F.; Maurya, M. R.; Azam, A. *Eur. J. Med. Chem.* **2006**, *41*, 592.
22. (a) Abid, M.; Azam, A. *Bioorg. Med. Chem.* **2005**, *13*, 2213; (b) Abid, M.; Bhat, A. R.; Athar, F.; Azam, A. *Eur. J. Med. Chem.* **2009**, *44*, 417.
23. Abid, M.; Agarwal, S. M.; Azam, A. *Eur. J. Med. Chem.* **2008**, *43*, 2035.
24. (a) Greenbaum, D. C.; Mackey, Z.; Hansell, E.; Doyle, P.; Gut, J.; Caffrey, C. R.; Lehrman, J.; Rosenthal, P. J.; McKerrow, J. H.; Chibale, K. *J. Med. Chem.* **2004**, *47*, 3212; (b) Biot, C.; Pradines, B.; Sergeant, M.-H.; Gut, J.; Rosenthal, P. J.; Chibale, K. *Bioorg. Med. Chem. Lett.* **2007**, *17*, 6434; (c) Oliveira, R. B.; de Souza-Fagundes, E. M.; Soares, R. P. P.; Andrade, A. A.; Krettli, A. U.; Zani, C. L. *Eur. J. Med. Chem.* **2008**, *43*, 1983; (d) Mallari, J. P.; Guiguemde, W. A.; Guy, R. K. *Bioorg. Med. Chem. Lett.* **2009**, *19*, 3546.
25. Scovill, J. P.; Klayman, D. L.; Franchino, C. F. *J. Med. Chem.* **1982**, *25*, 1261.
26. (a) Stump, B.; Kaiser, M.; Brun, R.; Krauth-Siegel, R. L.; Diederich, F. *ChemMedChem* **2007**, *2*, 1708; (b) Rodríguez-Argüelles, M. C.; Tourón-Touceda, P.; Cao, R.; García-Deibe, A. M.; Pelagatti, P.; Pelizzi, C.; Zani, F. *J. Inorg. Biochem.* **2009**, *103*, 21; (c) Moreira, D. R. M.; Leite, A. C. L.; Santos, R. R.; Soares, M. B. P. *Curr. Drug Targets* **2009**, *10*, 212.
27. Padhye, S.; Afrasiabi, Z.; Sinn, E.; Fok, J.; Mehta, K.; Rath, N. *Inorg. Chem.* **2005**, *44*, 1154.
28. Sharma, S.; Athar, F.; Maurya, M. R.; Azam, A. *Eur. J. Med. Chem.* **2005**, *40*, 1414.
29. Li, Q.; Tang, H.; Li, Y.; Wang, M.; Wang, L.; Xia, C. *J. Inorg. Biochem.* **2000**, *78*, 167.
30. Singh, V. P.; Katiyar, A.; Singh, S. *Biometals* **2008**, *21*, 491.
31. Singh, B.; Yadava, B.; Aggarwal, R. C. *Indian J. Chem.* **1984**, *23A*, 441.
32. Navarro, M.; Cisneros-Fajardo, E. J.; Sierralta, A.; Fernandez-Mestre, M.; Arrieche, P. S. D.; Marchan, E. *J. Biol. Inorg. Chem.* **2003**, *8*, 401.
33. Jones, R.; Summerville, D.; Basolo, F. *Chem. Rev.* **1979**, *79*, 139.
34. (a) Ferraz, K. S. O.; Ferandes, L.; Carrilho, D.; Pinto, M. C. X.; Leite, M. F.; Souza-Fagundes, E. M.; Speziali, N. L.; Mendes, I. C.; Beraldo, H. *Bioorg. Med. Chem.* **2009**, *17*, 7138; (b) Aghatabay, N. B.; Somer, M.; Senela, M.; Dulger, B.; Gucin, F. *Eur. J. Med. Chem.* **2007**, *42*, 1069.
35. Martinez, A.; Rajapakse, C. S. K.; Jalloh, D.; Dautriche, C.; Sanchez-Delgado, R. A. *J. Biol. Inorg. Chem.* **2009**, *14*, 863.
36. Espinosa, A.; Perdrizet, G.; Mino, G. P.; Phay, M. *J. Antimicrob. Chemother.* **2009**, *63*, 675.
37. Osullivan, D. G.; Sadler, P. W.; Webley, C. *Chemotherapia* **1963**, *7*, 17.
38. Price, J. H.; Williamson, A. N.; Schramm, R. F.; Wayland, B. B. *Inorg. Chem.* **1972**, *116*, 1280.
39. de Sá, M. S.; Costa, J. F. O.; Krettli, A. U.; Zalis, M. G.; Maia, G. L. A.; Sette, I. M. F.; Camara, C. A.; Filho, J. M. B.; Harley, A. M. G.; dos Santos, R. R.; Soares, M. B. P. *Parasitol. Res.* **2009**, *105*, 275.
40. Wright, C. W.; O'neill, M. J.; Phillipson, J. D.; Warhurst, D. C. *Antimicrob. Agents Chemother.* **1988**, *32*, 1725.
41. Diamond, L. S.; Harlow, D. R.; Cunnick, L. S. *Trans. R. Soc. Trop. Med. Hyg.* **1978**, *72*, 431.